

PAPR Reduction for AFDM by Affine-Domain Circular Shift without Side Information

The Khai Nguyen and Ebrahim Bedeer

Abstract—This paper proposes a novel method to reduce the peak-to-average-power-ratio (PAPR) of affine frequency division multiplexing (AFDM) signals without side information (SI). The method is based on circularly shifting the original transmit signal in the affine domain, and selecting the shifted candidate with the lowest PAPR. Next, a maximum-likelihood-based (MLB) receiver is derived, which exploits the position of the AFDM pilot and guard band to detect the shift applied at the transmitter without SI. Simulation results show that the proposed method can achieve 2.5 to 4 dB in PAPR reduction as compared to original AFDM and existing schemes, which can be translated into significantly lower error rate, depending on the quality of power amplifiers.

Index Terms—AFDM, PAPR reduction

I. INTRODUCTION

Affine frequency division multiplexing (AFDM) is a novel multicarrier technique that has gained increasing attentions recently [1], [2]. AFDM uses chirp-based waveforms derived from the discrete affine Fourier transform (DAFT), enabling joint time-frequency spreading of data symbols. Unlike orthogonal frequency division multiplexing (OFDM), which is susceptible to inter-carrier-interference due to Doppler effect and has poor diversity in doubly selective channel, AFDM can maintain full delay-Doppler diversity even under severe Doppler shift, making it ideal for high-mobility scenarios such as vehicular or satellite communications [1], [2]. However, like OFDM, AFDM exhibits high peak-to-average power ratio (PAPR), which motivates ongoing research on novel PAPR reduction methods suitable to AFDM.

In [3], the authors propose to vary the pre-chirp parameter c_2 across subcarrier groups in a non-enumerated way, and select the candidate with the lowest peak power. This method can achieve up to 5 dB lower PAPR than original AFDM, at the cost of higher complexity and rate loss due to side information (SI). In [4] the authors utilize μ -law companding to compress signal amplitude and limit peak power, while maintaining the Doppler resilience of AFDM. The paper derives an upper bound for PAPR and validates the approach through simulation, showcasing significant PAPR reduction compared to original AFDM (up to 4 dB). The work in [5] proposes a unified pre-modulation data-spreading algorithm to reduce the PAPR in AFDM systems without SI. This method uses different well-known transformations to redistribute signal energy before modulation, which demonstrates up to 4 dB PAPR reduction while maintaining spectral efficiency. In [6] a hybrid approach is introduced, which integrates Zadoff-Chu sequence matrix (ZCM) precoding with normalized μ -law and A -law companding to compress signal peaks while maintaining delay-Doppler diversity. The reported results show a moderate PAPR reduction and over 0.5 dB signal-to-noise ratio (SNR) improvement over conventional AFDM.

Despite the promising performances, the aforementioned works overlook the pilot structure of AFDM and how channel estimation could be affected [7]. To address this, the authors in [7] propose to replace the AFDM guard intervals with low-magnitude samples and jointly perform active constellation extension on data symbols, which is trained by a neural network using PAPR as the loss function. Although the non-zero guard band worsens channel estimation quality, the reported results show a notable PAPR reduction with minimal impact on bit error rate (BER), at the expense of higher complexity. The work in [8] selects the optimal value of c_2 that yields the lowest PAPR, from a predetermined set. The candidate set is chosen such that the applied c_2 value can be recognized at the receiver without SI, and does not affect the pilot structure of AFDM. The proposed approach was shown to achieve 2-3 dB PAPR reduction while improving BER performance compared to existing PAPR reduction schemes for AFDM.

Against the aforementioned background, in this paper, we propose a PAPR reduction method utilizing circular shift in the affine domain. The proposed method searches for the optimal circular shift that results in the lowest peak power among the candidate set. After that, a maximum-likelihood-based (MLB) blind detector is derived, which exploits the pilot structure of AFDM to detect the number of samples by which the original signal was circularly shifted at the transmitter, without SI. Next, we propose to limit the number of shifted candidates by applying a minimum spacing between any two different shifts, which helps reduce the error of the MLB blind detector due to the similarity between close candidates.

The remainder of this paper is organized as follows. Section II presents the system model and the proposed PAPR reduction method with affine-domain circular shift. Section III derives the blind estimation for the shift without SI. Section IV presents complexity analysis. Then Section V provides simulation results. Finally, Section VI concludes the paper.

Notations: The pairwise multiplication is \otimes . The circular convolution is \odot . Transposed and Hermitian matrices are denoted by the superscript T and H, respectively. Identity matrix of size N is \mathbf{I}_N . The modulo operator is mod. The set of $d_1 \times d_2$ complex matrices is $\mathbb{C}^{d_1 \times d_2}$. The central complex normal distribution with variance σ^2 is denoted by $\mathcal{CN}(0, \sigma^2)$. The circular shifts to the left and right are denoted by \ll and \gg , respectively. The determinant of a matrix is $\det(\cdot)$.

II. PAPR REDUCTION BY AFFINE-DOMAIN CIRCULAR SHIFT

A. System model

Consider an AFDM system with N subcarriers and the parameters c_1, c_2 . The input signal to the system in the affine domain $\mathbf{x} = [x[0], x[1] \dots x[N-1]]^T \in \mathbb{C}^{N \times 1}$ is drawn from

T. K. Nguyen and E. Bedeer are with the Department of Electrical and Computer Engineering, University of Saskatchewan, Saskatoon, Canada S7N5A9. Emails: {khai.nguyen, e.bedeer}@usask.ca.

This work was supported by the NSERC/Cisco Industrial Research Chair.

an M -QAM constellation. This signal is AFDM modulated into the time-domain signal $\mathbf{s} = [s[0], s[1] \dots s[N-1]]^T$ as:

$$s[n] = \sum_{m=0}^{N-1} \frac{x[m]}{\sqrt{N}} \exp \left\{ j2\pi \left[c_1 n^2 + \frac{mn}{N} + c_2 m^2 \right] \right\}. \quad (1)$$

This can be rewritten in the matrix form as:

$$\mathbf{s} = \mathbf{A}^H \mathbf{x} = \mathbf{\Lambda}_1^H \mathbf{F}^{-1} \mathbf{\Lambda}_2^H \mathbf{x}, \quad (2)$$

where $\mathbf{\Lambda}_i = \text{diag}(\exp(-j2\pi c_i n^2))$, (for $i \in \{1, 2\}$), and \mathbf{F} is the unitary discrete Fourier transform (DFT) matrix. Then, a chirp periodic prefix (CPP) is added to avoid inter-symbol-interference (ISI). After that, the signal is transmitted over a doubly selective channel with impulse response:

$$h[n, \tau] = \sum_{\ell=0}^{L-1} h_\ell \delta(\tau - \tau_\ell) \exp \{ j2\pi f_\ell n \}, \quad (3)$$

where L is the number of paths, $h_\ell \sim \mathcal{CN}(0, \rho_\ell)$ is the complex channel gain with variance ρ_ℓ , while τ_ℓ, f_ℓ are the delay and Doppler shift of the ℓ th path normalized by the sampling period. Without the loss of generality, we set $\tau_\ell = \ell - 1$, which means that the maximum delay is $\max(\tau_\ell) = L - 1$. With the use of a CPP to avoid ISI, the input-output signal relationship of AFDM signals over the channel after CPP removal is [1]:

$$\mathbf{r} = \mathbf{H}\mathbf{s} + \mathbf{w}, \quad (4)$$

where $\mathbf{w} \sim \mathcal{CN}(0, \sigma^2 \mathbf{I}_N)$ is AWGN noise and the channel matrix \mathbf{H} is defined as $\mathbf{H} \triangleq \sum_{\ell=1}^L h_\ell \mathbf{\Gamma}_p \mathbf{\Delta}_{f_\ell} \mathbf{\Pi}^{\tau_\ell}$, where

$$\mathbf{\Pi} = \begin{bmatrix} 0 & 0 & \dots & 0 & 1 \\ 1 & 0 & \dots & 0 & 0 \\ \vdots & \ddots & \ddots & \ddots & \vdots \\ 0 & 0 & \dots & 1 & 0 \end{bmatrix}, \quad (5)$$

$\mathbf{\Delta}_{f_\ell} = \text{diag}\{\exp\{j2\pi f_\ell n\}\}$, ($n = 0, 1 \dots N-1$) and $\mathbf{\Gamma}_p$ is an identity matrix when c_1 is set as [1]:

$$c_1 = \frac{2(\alpha_{\max} + \xi) + 1}{N}, \quad (6)$$

where the non-negative integer ξ is the spacing parameter. The received signal is converted back to the affine domain by [1]:

$$\mathbf{y} = \mathbf{A}\mathbf{r} = \mathbf{H}_{\text{eff}}\mathbf{x} + \tilde{\mathbf{w}}, \quad (7)$$

where $\mathbf{H}_{\text{eff}} \triangleq \sum_{\ell=0}^{L-1} h_\ell \mathbf{H}_\ell$ and $\mathbf{H}_\ell \triangleq \mathbf{A}\mathbf{\Gamma}_\ell \mathbf{\Delta}_{f_\ell} \mathbf{\Pi}^{\tau_\ell} \mathbf{A}^H$. Let the Doppler normalized to subcarrier spacing be defined as $\nu_\ell \triangleq N f_\ell = \alpha_\ell + a_\ell$, where α_ℓ is the integer part $\alpha_\ell \in [-\alpha_{\max}, \alpha_{\max}]$ and a_ℓ is the fractional part that satisfies $-0.5 < a_\ell \leq 0.5$. With c_1 defined as in (6), the full diversity of the channel is achieved [1]. The spacing parameter ξ is responsible for separating the channels of different paths in \mathbf{H}_{eff} to avoid overlapping among different paths (different \mathbf{H}_ℓ) that can degrade the diversity (with integer Doppler, $\xi = 0$).

B. PAPR reduction with affine domain circular shift

The PAPR of the AFDM modulated signal is defined as:

$$\text{PAPR}\{\mathbf{s}\} = \frac{\max(|s[n]|^2)}{\mathbb{E}\{|s[n]|^2\}}. \quad (8)$$

Let $\tilde{\mathbf{s}}_0 = \mathbf{F}^{-1} \mathbf{\Lambda}_2^H \mathbf{x} = \text{IDFT}\{\mathbf{a}_2 \otimes \mathbf{x}\}$, where $\mathbf{a}_2 = \text{diag}(\mathbf{\Lambda}_2^H) = \exp(j2\pi c_2 n^2)$. From (2), it can be seen that $\mathbf{s} = \mathbf{\Lambda}_1^H \tilde{\mathbf{s}}_0$, and thus, the multiplication with $\mathbf{\Lambda}_1^H$ simply makes \mathbf{s} a phase rotation of $\tilde{\mathbf{s}}_0$, which does not affect the sample power. Thus, it can be seen that:

$$\text{PAPR}\{\mathbf{s}\} = \text{PAPR}\{\tilde{\mathbf{s}}_0\}. \quad (9)$$

This simplifies the PAPR reduction problem since the parameter c_1 is removed. Then, we propose to transmit a circularly shifted version of \mathbf{x} that has a lower peak power, instead of the original \mathbf{x} . The search for the optimal shift will resort to choosing the one leading to the lower peak power:

$$\hat{k} = \underset{k=0,1,\dots,N-1}{\text{argmin}} \max\{|\text{IDFT}\{\mathbf{a}_2 \otimes (\mathbf{x} \gg k)\}|\} \quad (10)$$

Then, the signal $\tilde{\mathbf{x}}_{\hat{k}} \triangleq (\mathbf{x} \gg \hat{k})$ will be AFDM modulated by (2) and transmitted over the channel instead of \mathbf{x} .

In OFDM, a circular shift in the frequency domain only results in a phase shift in the time-domain signal, which does not change the PAPR. By contrast, in AFDM, circularly shifting \mathbf{x} before prechirping can change the PAPR of the AFDM in the time domain due to the multiplication with $\mathbf{\Lambda}_2^H$ in (2). With this method, the receiver needs to know the shift applied at the transmitter to revert the signal in the affine domain back to original. The use of SI as in many existing works in PAPR reduction is not applicable, since SI can only be extracted after the data has been detected, which is not possible without knowing how much \mathbf{x} has been shifted first. The channel estimation is also infeasible for the same reason. Thus, in the next section, we propose a blind estimation for the shift in the affine domain, without SI.

III. BLIND ESTIMATION OF AFFINE DOMAIN SHIFT

This section proposes a blind estimation method for the shift associated with PAPR reduction. Conventionally, AFDM requires a single pilot sample embedded in \mathbf{x} , surrounded by Q zero guard samples on each side of the pilot [1], where

$$Q = (\max(\tau_\ell) + 1) \times \beta - 1 = L\beta - 1, \quad (11)$$

with $\beta \triangleq 2\alpha_\xi + 1$, and $\alpha_\xi = \alpha_{\max} + \xi$. The pilot embedded signal in the affine domain is therefore given as:

$$\mathbf{x} = [P, 0 \dots 0, x[Q+1] \dots x[N-Q-1], 0 \dots 0], \quad (12)$$

where P is the pilot symbol.

Next, the effect of the channel \mathbf{H}_{eff} on the pilot-embedded signal \mathbf{x} needs to be examined. According to [1], by setting ξ properly, \mathbf{H}_{eff} has a special structure where each row (and column) is composed of $\max(\tau_\ell) + 1 = L$ adjacent segments, each corresponds to a different delay (from 0 to $L-1$) and has the length of β samples as shown in Fig. 1-(a). For the simplicity in explaining the effect of \mathbf{H}_{eff} on \mathbf{x} , assume that no data is transmitted ($\mathbf{x} = [P, 0, 0 \dots 0]$) as in Fig. 1-(b) and the receiver is noise-free. In this case, the received signal $\mathbf{y} = \mathbf{H}_{\text{eff}}\mathbf{x}$ will be exactly the first column of \mathbf{H}_{eff} , which also has the special structure with L adjacent segments of β samples, while the remaining samples are zeros as shown in Fig. 1-(c). These L segments total $L \times \beta$ samples, and is confined

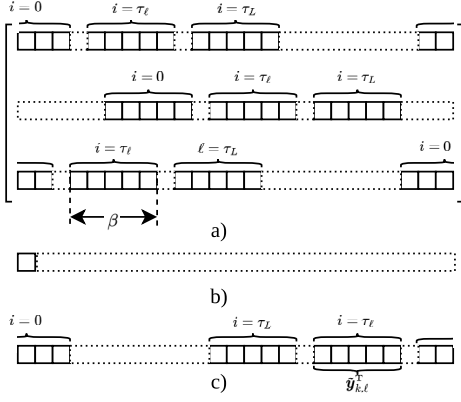


Fig. 1: Structure of: (a) \mathbf{H}_{eff} , (b) \mathbf{x}^T , and (c) $(\mathbf{H}_{\text{eff}}\mathbf{x})^T$.

completely within the guard interval of $2Q + 1$ samples of \mathbf{x} . More importantly, the remaining samples of the guard interval, which does not belong to any segments of any paths, guarantee that interference from data samples cannot reach any segments. This means that in a general case with pilot embedded plus data as in (12), the properties of these L segments analyzed earlier still hold, and are not affected by interference from data [1]. This is the most important establishment that enables the blind estimation of the shift for the proposed PAPR reduction.

For the ease in explanation, we will first start with the blind estimation of the shift for integer Doppler case. After that, the non-integer Doppler case can be addressed.

A. Integer Doppler case

As discussed earlier, with the parameters setting in (6), the channel with different delays or Doppler shifts are separated in the affine domain [1]. Consequently, when the pilot-embedded signal is transmitted, the L pilot-associated segments of $\mathbf{y} = \mathbf{H}_{\text{eff}}\mathbf{x}$, as shown in Fig. 1-(c), are mutually independent. Based on this, we will derive a MLB blind detector to determine if a segment of β samples taken from the received vector \mathbf{y} is associated with a channel path. Note that in the integer Doppler case, ξ is set to zero [1], which leads to $\beta = 2\alpha_{\text{max}} + 1$.

Suppose that the signal $\tilde{\mathbf{x}}_k = \mathbf{x} \gg k$ was transmitted, the position of the pilot will also be shifted by k samples (i.e. $\tilde{x}[k] = P$). Thus, to detect if the original signal \mathbf{x} was shifted to the right by k samples, the received signal \mathbf{y} will be circularly shifted to the left by k samples to obtain $\tilde{\mathbf{y}}_k = \mathbf{y} \ll k$. Let $\tilde{\mathbf{y}}_{k,\ell} \in \mathbb{C}^{\beta \times 1}$ be defined as $\tilde{\mathbf{y}}_{k,\ell} \triangleq [\tilde{y}_k[(-\ell\beta - \alpha_\xi) \bmod N] \dots \tilde{y}_k[(-\ell\beta + \alpha_\xi) \bmod N]]^T$, which are the β samples of the ℓ -th segment, given that $\tilde{\mathbf{x}}_k = \mathbf{x} \gg k$ was transmitted, as shown in Fig. 1-(c). Obviously, when the Doppler associated with this segment is $\alpha_\ell = 0$, the channel of the ℓ th tap will be at the central position of $\tilde{\mathbf{y}}_{k,\ell}$, i.e. $\tilde{y}_k[(-\ell\beta) \bmod N] = h_\ell$, while other samples are zeros. Whereas, when the Doppler is $\alpha_\ell = \pm 1$, the channel response of the ℓ th path will be shifted to the left and right by one sample, respectively. Generally, with integer Doppler, within $\tilde{\mathbf{y}}_{k,\ell}$, only one sample can be associated with the channel of the ℓ th tap $h_\ell \sim \mathcal{CN}(0, \rho_\ell)$, while the rest are just noise. Mathematically, with the integer Doppler α_ℓ :

$$\tilde{\mathbf{y}}_{k,\ell} \sim \mathcal{CN}(0, \text{diag}\{\mathbf{g}_{\alpha_\ell}\} + \sigma^2\mathbf{I}_\beta), \quad (13)$$

where $\mathbf{g}_{\alpha_\ell} = [g_{\alpha_\ell,1}, g_{\alpha_\ell,2}, \dots, g_{\alpha_\ell,\beta}]^T$ with all zero elements except $g_{\alpha_\ell,i} = \rho_\ell$ for $i = \alpha_{\text{max}} + 1 + \alpha_\ell$. Consequently, the the probability density function (pdf) of $\tilde{\mathbf{y}}_k$ conditioned on the integer Doppler shift α_ℓ is:

$$\Pr(\tilde{\mathbf{y}}_k|\alpha_\ell) = \frac{\exp\{-\tilde{\mathbf{y}}_{k,\ell}^H \Sigma_{\alpha_\ell}^{-1} \tilde{\mathbf{y}}_{k,\ell}\}}{(2\pi)^{\beta/2} \det\{\Sigma_{\alpha_\ell}\}}, \quad (14)$$

where $\Sigma_{\alpha_\ell} = \text{diag}\{\mathbf{g}_{\alpha_\ell}\} + \sigma^2\mathbf{I}_\beta$. Thus, the pdf of $\tilde{\mathbf{y}}_k$ is:

$$\Pr(\tilde{\mathbf{y}}_k) = \frac{1}{2\alpha_{\text{max}} + 1} \sum_{\alpha_\ell = -\alpha_{\text{max}}}^{\alpha_{\text{max}}} \Pr(\tilde{\mathbf{y}}_k|\alpha_\ell), \quad (15)$$

given that the Doppler is uniformly distributed. Finally, as discussed earlier that the segments associated with different paths are mutually independent, the likelihood that $\tilde{\mathbf{x}}_k = \mathbf{x} \gg k$ was transmitted can be calculated by taking the product of the pdfs of all segments averaged over their respective Doppler shifts. Then, the value of k with the highest likelihood will be decided as the shift applied at the transmitter:

$$\bar{k} = \underset{k=0,1,\dots,N-1}{\text{argmax}} \mathcal{L}(\tilde{\mathbf{x}}_k) = \underset{k=0,1,\dots,N-1}{\text{argmax}} \prod_{\ell=0}^{L-1} \Pr(\tilde{\mathbf{y}}_k). \quad (16)$$

B. Non-integer Doppler case

In the non-integer Doppler case, the response of the each channel path will not be centered at an exact integer-indexed bin in the affine domain. As a result, the channel response of the ℓ th path is spread over all samples of the ℓ th segment, and the AFDM modulator must employ a larger spacing to account for the spreading response (nonzero ξ) [1]. This modifies the distributions in (13) to

$$\tilde{\mathbf{y}}_{k,\ell} \sim \mathcal{CN}(0, \Psi_{\nu_\ell}), \quad (17)$$

where $\Psi_{\nu_\ell} = \rho_\ell \mathbf{b}_{\nu_\ell} \mathbf{b}_{\nu_\ell}^H + \sigma^2 \mathbf{I}_\beta$, and $\mathbf{b}_{\nu_\ell} = [b_{\nu_\ell}[0], b_{\nu_\ell}[1], \dots, b_{\nu_\ell}[2\xi]]^T$ and is given as in [1]:

$$b_{\nu_\ell}[i] = \frac{\exp\{-j2\pi(i - \xi - \nu_\ell)\} - 1}{\exp\{-j2\pi(i - \xi - \nu_\ell)/N\} - 1} \times \exp\{-j2\pi c_2((i - \xi) \bmod N)^2\}. \quad (18)$$

Proof: Without the loss of generality, the distribution of $\tilde{\mathbf{y}}_{k,\ell}$ can be calculated with $\ell = 0$ for simplicity, while remaining valid for all ℓ . As discussed earlier, $\tilde{\mathbf{y}}_{k,0}$ can be extracted from the first column of \mathbf{H}_{eff} as shown in Fig. 1. Since $\mathbf{H}_{\text{eff}} \triangleq \sum_{\ell=0}^{L-1} h_\ell \mathbf{H}_\ell$, and different \mathbf{H}_ℓ can be considered to have no non-zeros at the same positions [1], $\tilde{\mathbf{y}}_{k,0}$ are the non-zeros elements on the first column of $h_0 \mathbf{H}_0$, defined in [1] as:

$$H_\ell[p, q] = \frac{1}{N} \exp\{-j2\pi c_2 p^2\} \mathcal{F}_\ell[p, 0], \quad (19)$$

where $\mathcal{F}_\ell[p, q]$ is defined for non-integer Doppler in [1] as

$$\mathcal{F}_\ell[p, q] = \frac{\exp\{-j2\pi(p - q + 2Nc_1\tau_\ell + \nu_\ell)\} - 1}{\exp\{-j2\pi(p - q + 2Nc_1\tau_\ell + \nu_\ell)/N\} - 1}. \quad (20)$$

By substituting $\tau_0 = 0$, $q = 0$, the non-zero elements on the first column of \mathbf{H}_0 , which are from the $(N - \alpha_\xi)$ th to $(N - 1)$ th row and from 0th to the α_ξ th row can be obtained

as \mathbf{b}_{ν_0} in (18). As a result, the distribution of $\tilde{\mathbf{y}}_{k,0} = h_0 \mathbf{b}_{\nu_0}$ can be obtained as in (17). ■

Consequently, the pdf of $\tilde{\mathbf{y}}_k$ given that the Doppler of the ℓ -th tap is ν_ℓ is

$$\Pr(\tilde{\mathbf{y}}_k | \alpha_\ell) = \frac{\exp\left\{-\tilde{\mathbf{y}}_{k,\ell}^H \boldsymbol{\Psi}_{\nu_\ell}^{-1} \tilde{\mathbf{y}}_{k,\ell}\right\}}{(2\pi)^{\beta/2} \det\{\boldsymbol{\Psi}_{\nu_\ell}\}}. \quad (21)$$

Then, the likelihood that $\tilde{\mathbf{x}}_k = \mathbf{x} \gg k$ was transmitted is:

$$\mathcal{L}(\tilde{\mathbf{x}}_k) = \prod_{\ell=0}^{L-1} \left(\int_{-\alpha_{\max}-1}^{\alpha_{\max}+1} \Pr(\tilde{\mathbf{y}}_{k,\ell} | \nu_\ell) d\nu_\ell \right). \quad (22)$$

Evaluating this likelihood function is challenging due to the integral and the complex structure of $\boldsymbol{\Psi}_{\nu_\ell}$, which is dependent on the non-integer Doppler ν_ℓ . Thus, rather than directly evaluating (22) by solving the integral, we can instead approximate it with a Riemann sum. The sum can be evaluated by calculating the term $\Pr(\tilde{\mathbf{y}}_{k,\ell} | \nu_\ell)$ at some discrete, equally spaced frequencies of $\nu_\ell = k/G$, where k takes integer values (frequency step of $1/G$, where G is a positive integer). Then, the integral in (22) can be approximated with:

$$\tilde{\mathcal{L}}(\tilde{\mathbf{x}}_k) = \prod_{\ell=0}^{L-1} \left(\frac{1}{2\lambda+1} \sum_{k=-\lambda}^{\lambda} \Pr\left(\tilde{\mathbf{y}}_{k,\ell} \middle| \nu_\ell = \frac{k}{G}\right) \right), \quad (23)$$

where $\lambda = G(\alpha_{\max} + 1)$. By reducing the discrete frequency step (increasing G), the accuracy of the likelihood function can be improved, at the cost of higher complexity.

Note that the MLB detector derived above does not require CSI. Thus, after the shift has been detected, the received signal \mathbf{y} can be circularly shifted back to the original position, then the channel estimation can be performed normally as in [1].

C. Shift candidate spacing to reduce blind estimation error

It can be easily seen that the performance of MLB blind estimation derived above is strongly dependent on how distinguishable the positions of the pilot are with different shifts. For example, if the two shift candidates are only one sample apart (e.g. $k = 1$ and $k = 2$), the resulted positions of the pilot and the guard band are only different by one sample. As a result, $\tilde{\mathbf{x}}_1$ and $\tilde{\mathbf{x}}_2$ would be very similar, leading to likelihoods that are close in values. Thus, we propose to maintain a spacing of D samples between different candidates to reduce error. For example, with $D = Q$, the pilot band with different candidates can only be overlapped by only a half guard band (Q samples), which makes them more recognizable. In this simulation results, the effect of this spacing will be further illustrated and discussed. Consequently, the search for the optimal shift will be modified from (10) to:

$$\hat{k} = \underset{k=0, D, \dots, D \times \lfloor (N-1)/D \rfloor}{\operatorname{argmin}} \max\{|\operatorname{IDFT}\{\mathbf{a}_2 \otimes (\mathbf{x} \gg k)\}|\} \quad (24)$$

IV. COMPLEXITY ANALYSIS

The proposed method searches for the shifted candidate with the lowest PAPR to transmit. Thus, with $V = \lfloor N/D \rfloor$ candidates, where D is the spacing between to candidates with

the unit of sample, the total complexity for the PAPR reduction at the transmitter will be $\mathcal{O}(VN \log_2 N)$, which is V times higher than the conventional AFDM with no PAPR reduction.

On the other hand, the MLB detection requires the calculation of the pdf in (21) with the complexity of $\mathcal{O}((\alpha_{\max} + \xi)^2)$. Consequently, evaluating the likelihood function in (23), which requires the calculation of (21) for $\lambda = G(\alpha_{\max} + 1)$ discrete frequencies, L paths and V shift candidates requires the complexity of $\mathcal{O}(LVG(\alpha_{\max} + 1)(\alpha_{\max} + \xi)^2)$. Thus, the complexity of the receiver grows linearly with the number of taps, the size of the shift candidate set, and the number of discrete frequencies to calculate the likelihood functions in (23); while being a quadratic function of the maximum delay and frequency spacing parameter ξ . However, α_{\max} and ξ is usually of small values, which would not raise the complexity of the blind shift detection significantly, and hence, the complexity—no-SI trade-off can be justified.

V. SIMULATION RESULTS

This section provides simulation results to illustrate the merits of the proposed method in terms of the PAPR reduction capability and symbol error rate (SER) with a solid-state power amplifier (SSPA) with the smoothness parameter $\gamma = 3$, and the saturation (limit) amplitude A_{sat} varied proportionally to the standard deviation of the AFDM time domain signal σ_x [9]. The results are obtained with 16 QAM, the Doppler $\nu_\ell \in [-1, 1]$. The parameter c_2 is set at $2\pi/1000$, and the spacing parameter $\xi = 3$. The frequency step to calculate the likelihood function is $1/4$ ($G = 4$). The power of the pilot is set to $(2Q + 1)P_{\text{QAM}}$ to maintain the SNR of the time-domain signal equal to the SNR of the data on each subcarrier. The linear minimum mean squared error equalization will be used for data detection. The PAPR reduction performance will be evaluated based on the complementary cumulative density function (CCDF), which is defined as the probability that the PAPR is greater than PAPR_0 , mathematically $\Pr(\text{PAPR} \geq \text{PAPR}_0)$. The SER and PAPR performance of the proposed method is compared with the work in [8], which recently reports the best PAPR performance, does not require SI, and does not affect the channel estimation. According to [8], the optimal c_2 values for the lowest PAPR is exhaustively searched from a set of 8 candidates $\{\pm 1/N, \pm 2/N, \pm 3/M, \pm 4/N\}$.

Fig. 2 shows the PAPR of the proposed scheme with different candidate spacings. When the search is performed over all N shift candidates, the proposed method can achieve up to 4 dB gain at the CCDF of 10^{-4} , which is then reduced to 2.5 dB when the candidate spacing is expanded to $2Q$ samples. Moreover, with $D = Q/2$, the performance of the proposed method is equivalent to that of the reference method in [8].

As explained earlier, when the candidates are too close, the MLB blind detection cannot distinguish how much the position of the pilot has been shifted, which leads to higher SER. This can be seen in the SER comparison with $N = 256$ subcarriers in Fig. 3, where a candidate spacing of $D = \lfloor Q/2 \rfloor$ results in a very poor SER, reaching an error floor due to indistinguishable candidates. On the other hand, with $D = Q$ or $2Q$, the MLB shift detector can successfully estimate the shift, which results

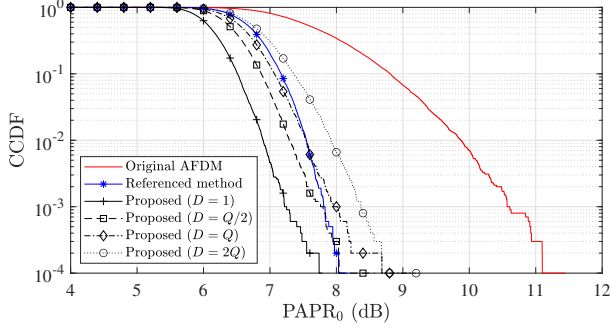


Fig. 2: PAPR with different candidate spacing ($N = 256$).

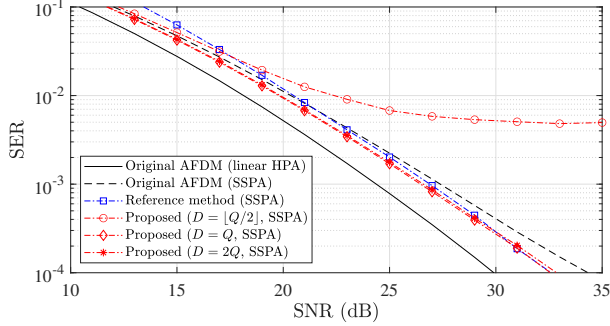


Fig. 3: SER with different candidate spacing ($N = 256$, $A_{\text{sat}} = 1.7\sigma_x$).

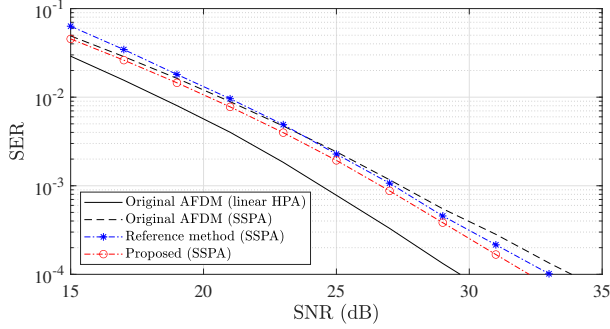


Fig. 4: SER comparison with [8] ($N = 512, A_{\text{sat}} = 1.7\sigma_x$, $D = Q$).

in roughly 2 dB gain over original AFDM without PAPR reduction (over SSPA) at the SER of 10^{-4} , equivalent to the performance of [8], while being 2.5 dB behind original AFDM with linear HPA. Whereas, with $N = 512$ subcarriers and $D = Q$ shown in Fig. 4, the proposed method can achieve a gain of roughly 1 dB over the method in [8] at the SER of 10^{-4} . This is due to the fact that with a higher number of subcarriers, while maintaining the same candidate spacing, the proposed method will have a bigger candidate set, which leads to improvement in PAPR, and hence, also an improvement in the SER as compared to [8].

Fig. 5 shows the SER performance when the quality of the SSPA varies. When the saturation level $A_{\text{sat}} = 2\sigma_x$, the performance of the propose scheme is almost identical to that of original AFDM with linear HPA, and is roughly 1 dB better than AFDM with no PAPR reduction at the SER of 10^{-4} . With $A_{\text{sat}} = 1.6\sigma_x$, this gap is significantly widen when the original AFDM is likely to approach an error floor due to

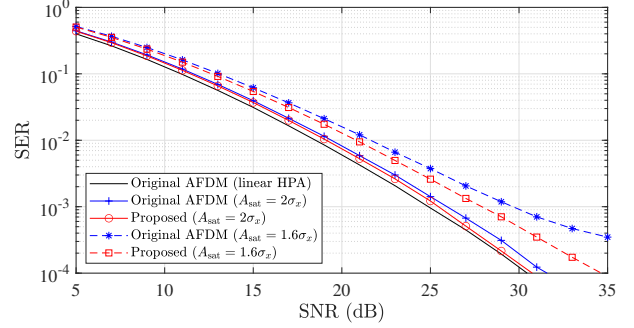


Fig. 5: SER with different SSPA qualities ($N = 256$, $D = Q$).

the non-linear distortion introduced by the HPA. Whereas, the proposed scheme can achieve a performance which is only 3 dB worse than the linear HPA case at the SER of 10^{-4} .

VI. CONCLUSIONS

This paper proposes a PAPR reduction method for AFDM signals based on circular shift in the affine domain. The method searches for the optimal number of samples that the original affine-domain signal needs to be circularly shifted to achieve the lowest PAPR before transmission. At the receiver, a MLB shift detection rule is derived, which exploiting the pilot embedded structure of AFDM symbols. The proposed ML-based blind detection can estimate the shift performed at the transmitter without SI, while not affecting the pilot structure of AFDM nor requiring CSI. As a result, the channel estimation can be performed as conventional after the shift is detected. To increase the reliability of the blind shift detector, we limit the number of shift candidates by maintaining spacing between candidates to make them more distinguishable at the receiver, which also helps reduce the search complexity for PAPR reduction purposes. Simulation results show that the proposed scheme can achieve around 2.5 to 4 dB in PAPR reduction, which is translated to up to 3 dB gain at the SER of 10^{-4} , depending on the SSPA quality.

REFERENCES

- [1] A. Bemani, N. Ksairi and M. Kountouris, "Affine frequency division multiplexing for next generation wireless communications," *IEEE Trans. Wireless Commun.*, vol. 22, no. 11, pp. 8214-8229, Nov. 2023
- [2] K. Zheng et al. "Channel estimation for AFDM with superimposed pilots," *IEEE Trans. Veh. Technol.*, vol. 74, no. 2, pp. 3389-3394, Feb. 2025.
- [3] H. Yuan et al., "PAPR reduction with pre-chirp selection for affine frequency division multiplexing," *IEEE Wireless Commun. Lett.*, vol. 14, no. 3, pp. 736-740, Mar. 2025
- [4] V. M. Reddy and H. Bitra, "PAPR in AFDM: Upper bound and reduction with normalized μ -law companding," *IEEE Access*, vol. 13, pp. 86553-86561, 2025.
- [5] A. Ali, A. Arous, and H. Arslan, "Spreading the wave: Low-complexity PAPR reduction for AFDM and OCDM in 6G networks," *IEEE Trans. Green Commun. Netw.*, vol. 10, pp. 1565-1577, 2026.
- [6] V. M. Reddy and H. Bitra, "PAPR reduction in AFDM using a Zadoff-Chu sequence matrix and companding transform," *IEEE Commun. Lett.*, vol. 30, pp. 847-851, 2026.
- [7] P. Huang et al., "Deep-learning-based PAPR reduction for pilot-embedded AFDM signals," *IEEE Commun. Lett.*, vol. 30, pp. 387-391, 2026.
- [8] K. Choi, "Low-PAPR AFDM with intrinsic SI and low complexity," *IEEE Wireless Commun. Lett.*, vol. 15, pp. 1494-1498, 2026.

- [9] C. Rapp, "Effects of HPA-nonlinearity on 4-DPSK/OFDM signal for a digital sound broadcasting system," in *Proc. 2nd European Conference on Satellite Communication*, 1991, pp. 179–184.